# REPORT DOCUMENTATION PAGE

*Form Approved*
*OMB No. 0704-0188*



**PLEASE DO NOT RETURN YOUR FORM TO THE ABOVE ADDRESS.**

| 1. REPORT DATE *(DD-MM-YYYY)* | 2. REPORT TYPE | 3. DATES COVERED *(From - To)* |
|---|---|---|
| 2008 | Reprint | Aug 2007-Aug 2008 |

**4. TITLE AND SUBTITLE**

THE EFFECT OF ADDED AL2O3 ON THE PROPAGATION BEHAVIOR OF AN Al/CuO NANOSCALE THERMITE

**5a. CONTRACT NUMBER**

W911NF-04-1-0178

**5b. GRANT NUMBER**

**5c. PROGRAM ELEMENT NUMBER**

**6. AUTHOR(S)**

J. Y. Malchi a, Richard A. Yetter a,*, T. J. Foley b, and Steven F. Son c

**5d. PROJECT NUMBER**

**5e. TASK NUMBER**

**5f. WORK UNIT NUMBER**

**7. PERFORMING ORGANIZATION NAME(S) AND ADDRESS(ES)**

a The Pennsylvania State University, University Park, PA, USA
b Los Alamos National Laboratory, Los Alamos, NM, USA
c Purdue University, West Lafayette, IN, USA

**8. PERFORMING ORGANIZATION REPORT NUMBER**

**9. SPONSORING/MONITORING AGENCY NAME(S) AND ADDRESS(ES)**

U. S. Army Research Office
P.O. Box 12211
Research Triangle Park, NC 27709-2211

**10. SPONSOR/MONITOR'S ACRONYM(S)**

**11. SPONSOR/MONITOR'S REPORT NUMBER(S)**

**12. DISTRIBUTION/AVAILABILITY STATEMENT**

Approved for public release; federal purpose rights.

**13. SUPPLEMENTARY NOTES**

The views, opinions and/or findings contained in this report are those of the author(s) and should not be construed as an official

**14. ABSTRACT**

Three types of experiments were performed on an Al/CuO nanoscale thermite to understand the effect of adding a diluent (40 nm Al2O3 particles) to the mixture: the constant volume pressure cell, the unconfined burn tray, and the instrumented burn tube. The addition of Al2O3 decreased the pressure output and reaction velocity in all three experiments. Burn tube measurements showed three reaction velocity regimes: constant velocity observed when 0% (633 m/s) and 5% (570 m/s) of the total weight is Al2O3, constant acceleration observed at 10% (146 m/s to 544 m/s over a distance of 6 cm) and 15% (69 m/s to 112 m/s over a distance of 6 cm) Al2O3, and an unstable, spiraling combustion wave at 20%Al2O3. The pressure measurements correlated to these three regimes showing a dropoff in peak pressure as Al2O3 was added to the system, with relatively no pressure increase observed when 20% of the total weight was Al2O3. Equilibrium calculations showed that the addition of Al2O3 to an Al/CuO mixture lowered the flame temperature, reducing the amount of combustion products in the gas phase, thus, hindering the presumed primary mode of forward heat transfer, convection

**15. SUBJECT TERMS**

Burning rate; Diluent; Nano-aluminum; Thermite

| 16. SECURITY CLASSIFICATION OF: | | | 17. LIMITATION OF ABSTRACT | 18. NUMBER OF PAGES | 19a. NAME OF RESPONSIBLE PERSON |
|---|---|---|---|---|---|
| a. REPORT | b. ABSTRACT | c. THIS PAGE | | | Richard A. Yetter |
| UU | UU | UU | UU | 19 | 19b. TELEPHONE NUMBER *(Include area code)* 814-863-6375 |

Reset

**Standard Form 298** (Rev. 8/98)
Prescribed by ANSI Std. Z39.18


**Combustion Science and Technology**
Publication details, including instructions for authors and subscription information:
http://www.informaworld.com/smpp/title~content=t713456315

# The Effect of Added $Al_2O_3$ on the Propagation Behavior of an Al/CuO Nanoscale Thermite

J. Y. Malchi [a]; R. A. Yetter [a]; T. J. Foley [b]; S. F. Son [c]
[a] The Pennsylvania State University, University Park, PA, USA [b] Los Alamos National Laboratory, Los Alamos, NM, USA [c] Purdue University, West Lafayette, IN, USA

Online Publication Date: 01 July 2008

**To cite this Article** Malchi, J. Y., Yetter, R. A., Foley, T. J. and Son, S. F.(2008)'The Effect of Added $Al_2O_3$ on the Propagation Behavior of an Al/CuO Nanoscale Thermite',Combustion Science and Technology,180:7,1278 — 1294
**To link to this Article: DOI:** 10.1080/00102200802049471
**URL:** http://dx.doi.org/10.1080/00102200802049471

*Combust. Sci. and Tech.*, 180: 1278–1294, 2008

ISSN: 0010-2202 print/1563-521X online
DOI: 10.1080/00102200802049471

Taylor & Francis
Taylor & Francis Group

# THE EFFECT OF ADDED $Al_2O_3$ ON THE PROPAGATION BEHAVIOR OF AN Al/CuO NANOSCALE THERMITE

**J. Y. Malchi[1], R. A. Yetter[1], T. J. Foley[2], and S. F. Son[3]**
[1]*The Pennsylvania State University, University Park, PA, USA*
[2]*Los Alamos National Laboratory, Los Alamos, NM, USA*
[3]*Purdue University, West Lafayette, IN, USA*

***Three types of experiments were performed on an Al/CuO nanoscale thermite to understand the effect of adding a diluent (40 nm $Al_2O_3$ particles) to the mixture: the constant volume pressure cell, the unconfined burn tray, and the instrumented burn tube. The addition of $Al_2O_3$ decreased the pressure output and reaction velocity in all three experiments. Burn tube measurements showed three reaction velocity regimes: constant velocity observed when 0% (633 m/s) and 5% (570 m/s) of the total weight is $Al_2O_3$, constant acceleration observed at 10% (146 m/s to 544 m/s over a distance of 6 cm) and 15% (69 m/s to 112 m/s over a distance of 6 cm) $Al_2O_3$, and an unstable, spiraling combustion wave at 20% $Al_2O_3$. The pressure measurements correlated to these three regimes showing a dropoff in peak pressure as $Al_2O_3$ was added to the system, with relatively no pressure increase observed when 20% of the total weight was $Al_2O_3$. Equilibrium calculations showed that the addition of $Al_2O_3$ to an Al/CuO mixture lowered the flame temperature, reducing the amount of combustion products in the gas phase, thus, hindering the presumed primary mode of forward heat transfer, convection.***

***Keywords***: Burning rate; Diluent; Nano-aluminum; Thermite



## INTRODUCTION

A thermite reaction is defined as a reaction between a metal and a metal oxide (Wang et al., 1993). This work was focused on the metal-metal oxide reaction, not intermetallics (another name for metal-metal reactions). Using aluminum as the metal fuel with different oxidizers creates highly exothermic reactions that have applications in many areas associated with self-propagating high temperature

Received 16 January 2007; acceped 19 December 2007.

Authors are supported by Los Alamos National Laboratory (LANL), which is operated for the U.S. Department of Energy under the contract *DE-AC52-06NA25396*. Work was supported by the Joint DoD/DOE Munitions Program under the supervision of Sherri Bingert and the U.S. Army Research Office under the Multi-University Research Initiative under Contract No. W911NF-04-1-0178. The authors give a special thank you to Adam Pacheco and Dave Oschwald for their help setting up and running the equipment that made this study possible. For his help interpreting pressure transducer results, Dr. Patrick Walter of Texas Christian University is thanked as well. This work has been assigned LA-UR #07-7888.

Address correspondence to R. A. Yetter, 111 Research Bldg. East, University Park, PA 16802. E-mail: ray8@psu.edu

synthesis (SHS) (Wang et al., 1993) and energetic materials (Naud et al., 2003; Pantoya et al., 2004).

Burning velocities for these materials have been shown to be highly dependent on the particle size (Pantoya and Granier, 2005), whereby smaller particles lead to faster burning rates. Thermites with particle sizes on the nanoscale, also referred to as metastable interstitial composites (MICs), can exhibit burning rates up to 1000 m/s (Bockmon et al., 2005). The high burning rates and exothermicity makes these materials of great interest to the combustion community.

One aspect of MIC materials that is not well understood is the mode by which energy is transferred ahead of the reaction front to sustain the propagation, or the propagation mechanism. Five propagation mechanisms may be considered when examining the reaction propagation: radiation, conduction, acoustics, compaction, and convection (Asay et al., 2004). Solid energetic materials are controlled by conduction, when deflagrating, which can be enhanced by radiation (Son and Brewster, 1995; Begley and Brewster, 2007). Acoustics (shock processes) and compaction become important when a reaction produces pressures sufficient to induce volume changes in the material. This occurs during detonation or the transition to detonation. Convection is possible if the material is porous and hot interstitial gas, reactants, or products can be propelled forward through the material by high reaction zone pressures (Kuo et al., 1978; Ershov et al., 2001).

Nanoscale thermites exhibit combustion velocities ($\sim$1000 m/s) approximately four orders of magnitude greater than that of the micron-scale thermites ($\sim$0.1 m/s) (Bockmon et al., 2005 and Wang et al., 1993). The drastic increase in velocity is due to the extremely small time scales associated with mass diffusion and reaction rates brought about by the small particle sizes. This does not allow time for any heat loss or depressurization within the reaction zone leading to high pressure, hot gases that can be propelled ahead of the front. Therefore, these systems are thought to be controlled by a convective propagation mechanism (Asay et al., 2004).

Because the controlling propagation mechanism is convection, both gas production and temperature, should be important factors when optimizing for the fastest burning rate. Sanders et al. (2006) observed that for four different metal oxides ($Bi_2O_3$, $MoO_3$, CuO, and $WO_3$), the burning rate on a burn tray was maximized at the stoichiometry that also produced the highest peak pressure in the pressure cell. Moreover, equilibrium calculations showed that all of the optimum stoichiometric ratios were related to the gas production and phase of the products. This optimum stoichiometry was found to be fuel rich ($\sim$1.4) for all of the metal oxides except copper oxide, which optimized at an equivalence ratio close to 1. This difference was attributed to the fact that one of the main products, copper, has a relatively high boiling point of 2835 K and needed the high temperature of a stoichiometric reaction to keep it in the gas phase. This work focused on the reaction of nano-aluminum (nAl) with copper oxide. The global reaction is

$$2Al + 3CuO \rightarrow Al_2O_3 + 3Cu \quad \Delta H_r = -4.08 \text{ kJ/g} \tag{1}$$

where $\Delta H_r$ is the heat of reaction based on the mass of the reactants.

Similar to varying the stoichiometry, adding a diluent into the system will decrease the overall temperature of the reaction. Adding the end product, particularly $Al_2O_3$, as a diluent was a common practice in micron-scale thermite SHS in order to reduce combustion temperatures and change the mechanical properties of the products (Varma et al., 1992; Munir and Anselmi-Tamburini, 1989). Moreover, the decrease in combustion temperature gave way to slower reaction velocities and decreasing amounts of gaseous species (Wang et al., 1993).

This work focused on the effects of dilution on the combustion properties of the Al/CuO nano-scale thermite. Alumina nano-particles were added in given percentages and their effect on pressure and reaction velocity was studied. A similar study was performed with an $Al/MoO_3$ system by Foley et al. (2006) from which comparisons are made. The global reaction for this thermite system is given in Eq. (2).

$$2Al + MoO_3 \rightarrow Al_2O_3 + Mo \quad \Delta H_r = -4.70 \text{ kJ/g} \tag{2}$$

The authors hypothesized that the dilution will lower combustion temperatures, which will decrease gas production and, thus hinder the convective propagation mechanism.



## EXPERIMENT

Three experiments were performed to characterize the effects of adding a diluent ($Al_2O_3$ nano-particles) to an Al/CuO nanoscale thermite or MIC. The pressure cell gave pressure traces for a constant volume explosion, the burn tray yielded a two-point velocity of the reaction propagating through the unconfined material, and the burn tube provided information about the pressure and reaction velocity in confined conditions. Brief descriptions are given here, but detailed experimental descriptions can be found in Sanders et al. (2006).

### Materials and Material Preparation

Note: Care should be exercised and small amounts of material used when handling the formulated composites because of their sensitivity to impact, spark, and friction.

Nano-aluminum was purchased from *Nanotechnologies Inc.* (currently, Novacentrix Inc.) and had a nominal particle size of 80 nm with 88% active aluminum (Mang et al., 2006). Particles were assumed to all have a spherical geometry. Copper oxide particles were purchased from Technologies Inc. with all particles assumed to have cylindrical geometry with dimensions of 21 nm $\times$ 100 nm. Assumptions on particle geometries are from SEM analysis of the Al and CuO particles (Fig. 1). The alpha-aluminum oxide ($Al_2O_3$) particles were purchased from *Nanotechnologies Inc.* and had a nominal particle size of 40 nm.

All composites had a ratio of 22% nAl and 78% CuO by mass which is based on the optimization from Sanders et al. (2006). Alumina was added to this system in increments to produce the desired dilution (increments are labeled as percentage of *added* alumina, thus the overall alumina percentage will be higher due to the inherent

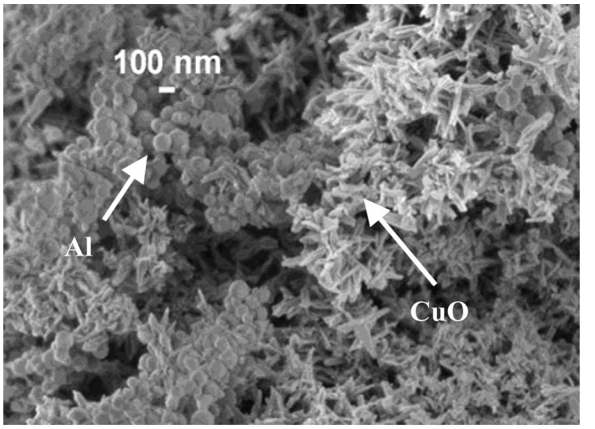


**Figure 1** SEM of Al/CuO nanoscale thermite at 25K× magnification.



alumina shell on the nAl). Mixtures were combined in glass vials and slurried in ~12 ml of hexanes. The slurry was sonicated for a total of 1 minute in 0.5 s intervals (50% duty-cycle) at 200 W using a *Heat Systems XL 2020* sonicator. It was then placed in a steel pan and dried on a hot plate at ~48°C for ~10 minutes (until material appeared dry). The material was then sieved through a 355μm mesh to break up any large agglomerates.

### Pressure Cell

A modified Parr bomb was used to acquire constant volume pressure traces (Perry et al., 2004). Ignition was achieved by pulsing a 1064 nm Nd:YAG laser (~9 mJ) onto the material in the cell via an optical fiber. The free volume of the cell was 13 $cm^3$ and the appropriate amount of material was placed in a cup resting at the bottom of the cell. Pressure measurements were taken at the wall of the cell using a *PCB Piezotronics* piezoelectronic pressure transducer with a *PCB Piezotronics* signal-conditioner (model 482A20). Data were recorded at 10 MHz with a *National Instruments* PCI-6115 data acquisition board (DAQ). The q-switch from the laser was used to trigger the data acquisition system.

The mass of MIC material placed in the cup remained a constant value of 17.5 mg irrespective of the amount of added diluent in the system to keep the energy content constant. For example, if an experiment was being performed on a sample with 5% added $Al_2O_3$ nano-particles, the amount of MIC would be 17.5 mg (22% by mass nAl including oxide passivation, and 78% CuO), but the total mass of material in the cup would be 18.42 mg.

### Burn Tray

A loose sample of material (50 mg) was lined up on a metal tray to measure an unconfined reaction velocity (Perry et al., 2004). Two holes, ~1 mm in diameter, were 20 mm apart on the base of the metal tray, on top of which the material was

placed. Two optical fibers were placed in these holes and attached on their other end to a *Thorlabs* DET-210 photodiode to detect light emission from the reaction at the beginning and end of the line of material. The distance and time between these two light signals were used to find a two-point velocity. The light from the first photodiode was also used as a trigger for the DAQ system. The data were collected by the same DAQ system described in the previous section. Material ignition was achieved by piezoelectric discharge.

### Burn Tube

The burn tube experiment originally designed and used by Bockmon et al. (2005) was used in this experiment with some modifications. This experiment gave a means of measuring the reaction velocity in a confined, more one-dimensional, cylindrical geometry. An acrylic tube used to hold the material, with length of 8.9 cm, inner diameter of 0.32 cm, and outer diameter of 0.64 cm, was placed in a polycarbonate block. Six pressure transducers and optical fiber ports were located on each side of the block at 1 cm intervals.

Materials were loaded into acrylic tubes using a *Cleveland* vibrating block to assure uniform powder density. Packing densities were approximately 6% of the theoretical maximum density (TMD), which corresponded to 250 mg per experiment or $0.36\,g/cm^3$. Initiation of the reaction was achieved by means of an exploding bridge wire (EBW), which was placed at one end of the tube and fired by a *Cordin* 640 Pulsor at 1.7 kV. A *Stanford Research Systems* pulse generator was used to manually trigger the Pulsar and DAQ system. The signal from the pulse generator corresponds to $t = 0$ in the experiments. For these experiments two *Tektronix* digital oscilloscopes (models 754D and 7054) with sampling rates of 5 MHz (0.2 μs resolution) were used to acquire the data.

A *Phantom 7.0* high-speed video camera was used to view the luminosity from the reaction wave propagating down the tube. A frame rate of 110,000 frames per second was used at a pixel resolution of $256 \times 32$ and exposure time of 1 μs. An appropriate aperture was chosen depending on the experiment to view the reaction without saturation. The pulse generator triggered the camera as well.

## RESULTS

Three tests were performed to characterize the effects of added $Al_2O_3$ nanoparticles on the burning rate of an Al/CuO nanoscale thermite: the pressure cell, the burn tray, and the burn tube. Both the pressure cell and the burn tray gave information about an unconfined burn while the burn tube was in a confined setup. Confinement effects were expected to play a significant role because the convective mode of heat transfer was the controlling propagation mechanism.

### Pressure Cell and Burn Tray

A single pressure trace was recorded in the pressure cell for each experiment. Typical results are shown in Figure 2 for varying weight percent of $Al_2O_3$. Below 5% added $Al_2O_3$, ringing was seen in the record. This was interpreted as shock waves

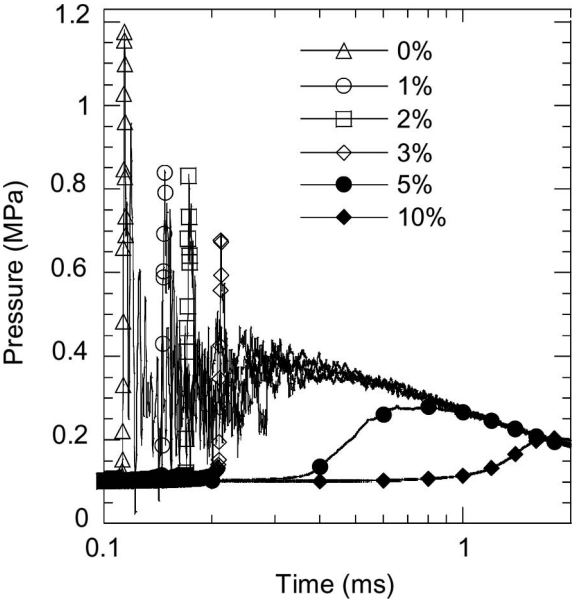


**Figure 2** Typical pressure traces from the pressure cell for increasing amounts of $Al_2O_3$. Data labels shown only on initial pressure rise for each trace.

reflecting off the walls inside the cell. A drastic change occurred in the pressure traces when 5% $Al_2O_3$ was added to the mixture whereby the peak pressure and rate of pressure rise (dP/dt) significantly decreased and the induction time ($\tau_i$) significantly increased.

The rate of pressure rise was defined as the difference between the peak pressure and atmospheric pressure divided by the difference between the time of peak pressure and the time where the pressure first rises above atmospheric conditions. Induction time was defined as the time from when the ignition energy was delivered to when the pressure rises above 10% of the peak pressure. Moreover, above 5% added $Al_2O_3$ there was no ringing in the pressure trace indicating the reaction was slowed to the point that a shock wave was not produced in the gas surrounding the sample.

The $Al/MoO_3$ system used in Foley et al. (2006) showed a similar drastic change in behavior for the rate of pressure rise and induction time at 20% added $Al_2O_3$ (compared to 5% for the Al/CuO system), which indicated that the Al/CuO CuO system was more sensitive to the addition of $Al_2O_3$. The peak pressure for the $Al/MoO_3$ system using 19 mg, however, was relatively low (0.33 MPa) compared to the Al/CuO system (1.17 MPa) for the sharp rising pressure traces (low percentage of $Al_2O_3$).

The pressure traces were fairly repeatable for each $Al/CuO/Al_2O_3$ case, except for the 4% case indicating the system was on the threshold of a change. The 4% case was not shown due to its extremely high variability in results. Specifically, some results in this range showed a sharp pressure rise with ringing and some resulted in a more monotonic rise in pressure similar to conditions where more $Al_2O_3$ was

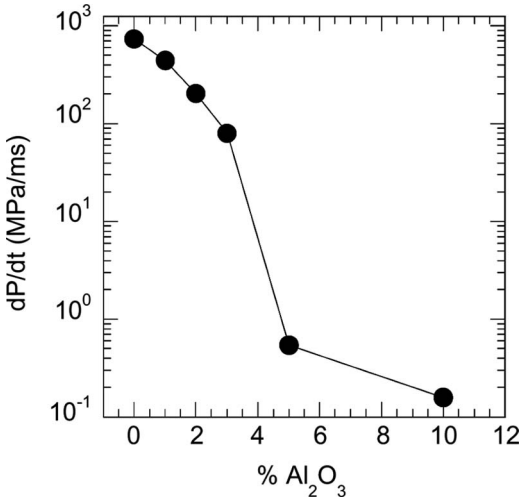


**Figure 3** Rate of pressure rise in the pressure cell with increasing weight percentages of $Al_2O_3$.

added. This distinct transition was indicative of a change in the mode of reaction propagation occurring.

Three experiments were performed for each weight percentage of $Al_2O_3$ in the pressure cell and values of peak pressure, dP/dt and $\tau_i$ were averaged. Figures 3 and 4 show the trends of dP/dt and $\tau_i$, respectively. The slope of the pressure rise dropped two orders of magnitude when the $Al_2O_3$ weight percentage increased from 3% to 5%, showing two different regimes. The induction time also showed a

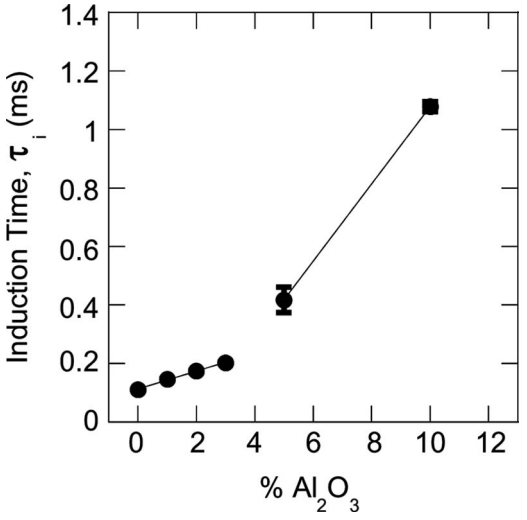


**Figure 4** Induction time ($\tau_i$) for the pressure rise in the pressure cell with increasing weight percentage of $Al_2O_3$.

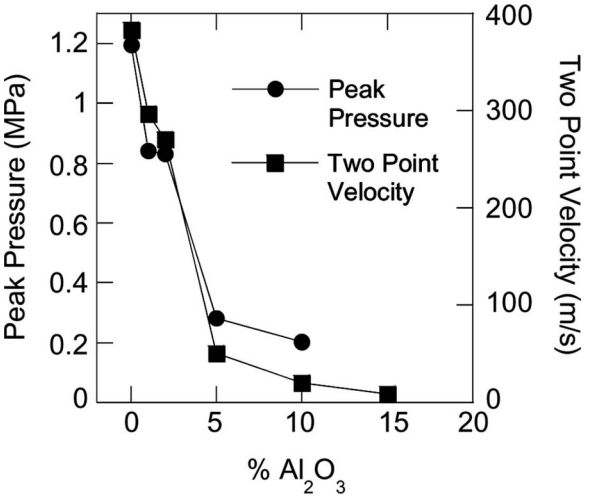


**Figure 5** Peak pressure in Parr bomb and open tray velocity result. There is a clear correlation between peak pressure in the pressure cell and two-point velocity on the burn tray with increasing weight percentages of $Al_2O_3$.



bimodal nature with a significant increase at 5%. Error bars representing a 95% confidence interval are present for all points, although some are hidden by their respective label.

The trend for the peak pressure, when varying the weight percent of $Al_2O_3$, was similar to that for the two-point velocity in the burn tray experiment as shown in Figure 5. For both, there was an initial drop of $\sim$27% in either peak pressure or velocity with only 1% $Al_2O_3$ added and then a drastic dropoff of $\sim$75% at 5% $Al_2O_3$. In contrast, Foley et al. (2006) observed a linear decrease in peak pressure and a change of regimes for velocity at 20% $Al_2O_3$ (Al/$MoO_3$ system). Error bars representing a 95% confidence interval are present, but smaller than the data point labels. The correlation between the pressure and velocity was also shown in Sanders et al. (2006) for various stoichiometric ratios. This gave further evidence that the propagation mechanism was closely related to the effects of pressure or gas production.

There was a limit to the amount of $Al_2O_3$ that could be added to the system for each test. The material in the pressure cell would not ignite with 15% by weight of $Al_2O_3$ by laser, nor in the burn tray with 20% $Al_2O_3$ using a piezo-igniter. In contrast, the Al/$MoO_3$ from Foley et al. (2006) was ignitable with 50% $Al_2O_3$ using the same ignition systems. The burn tray experiment had a higher threshold for $Al_2O_3$ because the ignition systems were different and more material was used and less was in contact with its container promoting more heat generation and less heat losses.

## Burn Tube

As was shown with the pressure cell and burn tray, this material was particularly sensitive to the addition of $Al_2O_3$. An addition of only 5% by weight of

$Al_2O_3$ in the mixture drastically changed the pressure output and propagation behavior. Both of these tests were unconfined, allowing some of the interstitial and combustion product gases to leave the system. The burn tube, however, confined the material laterally so all of the gas remained in the system, with some being propelled forward through the interstitial spaces. The photodiodes detected the light given off by the reaction while the pressure transducers detected the pressure change caused by the heating of the interstitial gases and the gas produced by the reaction.

*Light measurements.* Six photodiodes recorded the light production in the burn tube each separated by 1 cm. Figure 6 shows a typical sequence of images and light traces from a single experiment. Knowing the distance of each light detector and the time of arrival for the light trace, a position versus time plot and, thus a velocity could be acquired for each experiment. Multiple experiments were performed and averaged for each $Al_2O_3$ weight percentage. Both the position and time were zeroed at the first position since this study was not concerned with ignition effects. Figure 7 shows a typical graph of position vs. time for each $Al_2O_3$ percentage. The 0% and 5% experiments were nearly linear indicating a constant velocity; while the 10% and 15% had a second order polynomial fit indicating a non-steady velocity or constant acceleration.

The average velocities for the 0% and 5% cases were $633\,m/s \pm 7\%$ and $570\,m/s \pm 5\%$, respectively. The average accelerations for the 10% and 15% cases were $2{,}798{,}400\,m/s^2 \pm 30\%$ and $76{,}686\,m/s^2 \pm 17\%$, respectively. The initial and final velocities (from the fit) for the 10% added $Al_2O_3$ case, were 146 m/s and 544 m/s, respectively. Likewise, for the 15% added $Al_2O_3$ case, the initial and final velocities (from the fit) were 69 m/s and 112 m/s, respectively. The error represents a 95% confidence interval for a small sample. The $Al/MoO_3$ system first showed non-steady velocity at 50% $Al_2O_3$ (Foley et al., 2006).

For the experiment with 20% $Al_2O_3$ not all of the photodiodes recorded light during the experiment. This indicated that the reaction did not pass through the material covering that particular fiber optic and, therefore, the front was not continuous, but consisted of various discrete fronts, or fingers, propagating through

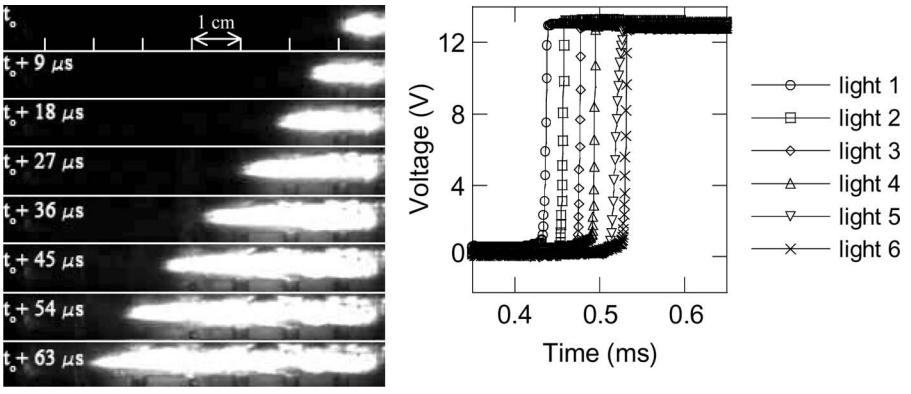


**Figure 6** Typical sequence of images and light traces from an experiment with 5% $Al_2O_3$.

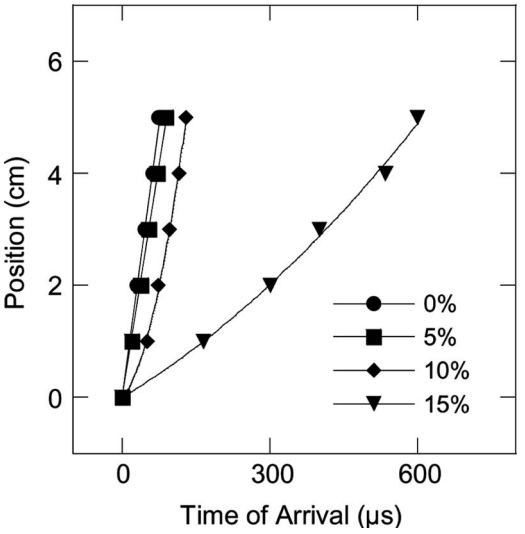


**Figure 7** Typical position versus time graphs for reaction waves in the burn tube with various weight percentages of $Al_2O_3$.

the material. In fact, images of this experiment in Figure 8 show a completely different flame structure spiraling through the material similar to, but not exactly the same as what was observed by Munir and Anselmi-Tamburini (1989) for diluted classical thermites.

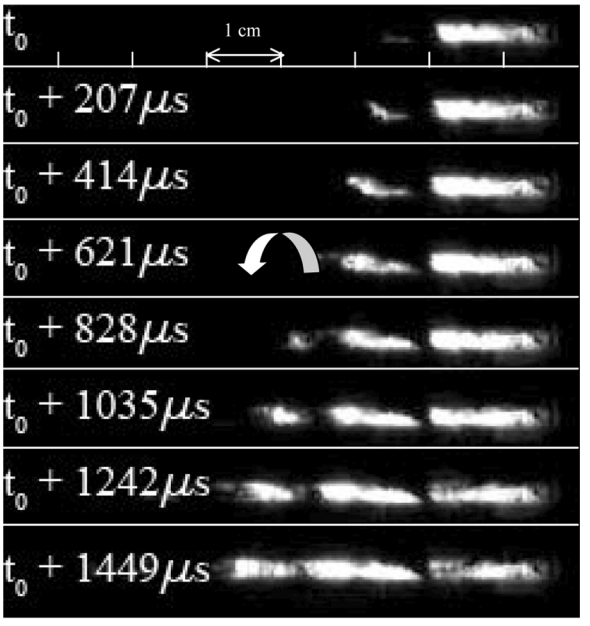


**Figure 8** Spiraling combustion instability shown.

This instability was attributed to the diluent decreasing the flame temperature and causing a thermal instability. The spiraling instability observed by Munir and Anselmi-Tamburini (1989) was different in that most of the material was consumed. Moreover, the samples were packed pellets as opposed to loose powder in a tube and the constituents used were not Al/CuO. Preceding this spiraling combustion, a flat and steady, but relatively slow front was observed to have speeds of $\sim 5\,\mathrm{m/s}$. This will be discussed further after examining the pressure traces for these unstable experiments.

*Pressure measurements.* The pressure transducers measured the change in pressure at a particular point due to the reaction forming hot gases and heating up the interstitial air. Ideally, these traces would be flat until the reaction reached the face of the transducer, and would then show a sharp pressure rise with a relatively slow decay as was shown with other experiments (Bockmon et al., 2005; Foley et al., 2006; Sanders et al., 2006). For this experiment, however, at 0% and 5% $Al_2O_3$, the traces were not as ideal. Even though most traces showed the discrete pressure rise, some had oscillations prior to the sharp pressure rise. Drops in the pressure to approximately $-2$ MPa (Fig. 9) were seen, which is due to equipment malfunction (a pressure of $-2\,\mathrm{MPa}$ relative to atmospheric pressure indicates an overall negative pressure).

Some traces did not have a sharp pressure rise at all and just oscillated around zero with an amplitude of approximately $\pm 2 - 7\,\mathrm{MPa}$. These were usually found at the 5th and 6th pressure transducer positions and maybe associated with effects from the open end of the tube. The time scale for these drastic pressure drops and

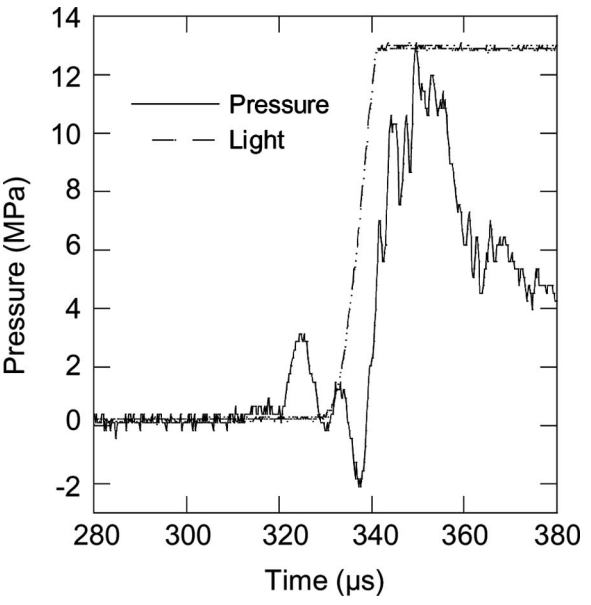


**Figure 9** Example of pressure rise before light trace and extreme negative pressure oscillation.

oscillations was $\sim 5\,\mu s$, which was too fast to attribute to thermal effects on the pressure transducers. Therefore, this could only be due to mechanical or electrical effects. This issue has not yet been resolved. Because of these unknown inconsistencies in the data, the pressure traces were not used to find a particular reaction velocity, but rather as a measure of the gas production in the system and heating of the interstitial air.

The experiments with 0% and 5% added $Al_2O_3$ gave peak pressures of $\sim 10\,MPa$ and $\sim 9\,MPa$, respectively, for most positions down the tube. However, at 10% added $Al_2O_3$, where the reaction wave velocity became unsteady (constant acceleration), most of the positions showed relatively low peak pressures, $\sim 2\,MPa$, and only a few positions showed pressures between 6 and 8 MPa. Figure 10 shows pressure traces from the 2nd and 5th position of a particular experiment with 10% $Al_2O_3$ demonstrating this bimodal behavior.

In this particular experiment, the pressure, or gas production, showed a drastic increase at the end of the tube giving an explanation for the accelerating front. The slow reaction in the beginning stages built up gases that would eventually propel the reaction forward and give it this constant acceleration. Presumably, it would eventually reach a steady propagation rate. Similar trends for the pressure were seen for 15% added $Al_2O_3$ with fewer positions showing pressures of $\sim 8\,MPa$. For 20% added $Al_2O_3$, pressure rises of $\sim 2\,MPa$ occurred at all pressure locations for all experiments indicating a significantly lower temperature reaction and more condensed phase combustion products. Much lower gas production for this experiment could be the reason for the slow and highly unstable reaction front.



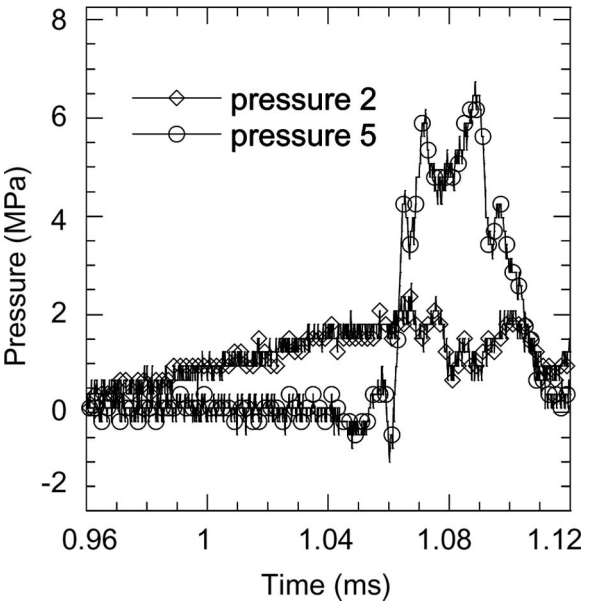


**Figure 10** Pressure traces at position 2 and 5 for an experiment with 10% $Al_2O_3$ showing the bi-modal characteristic with the high peak pressures at the later positions down the tube.

As $Al_2O_3$ was added to the system, the reaction in the burn tube changed from a steady rate (0% and 5% by weight), to an accelerating regime (10% and 15%), and finally, to an unstable regime (20%) where a relatively slow burning velocity was observed, which eventually transitioned to a spiraling combustion wave. The pressure traces gave indication that the gases being produced by the hot reaction, such as vaporized aluminum, unstable intermediates such as AlO or $Al_2O$ or stable products such as Cu gas, were condensing or not even forming due to the lower adiabatic flame temperatures. Therefore, this did not allow for hot gases to be propelled forward to drive the reaction down the tube convectively. This all occurred at lower levels of $Al_2O_3$ compared to the $Al/MoO_3$ system.

## Thermodynamics

Equilibrium calculations were performed using CHEETAH 4.0 (Fried et al., 2004) with the JCZS product library developed by Hobbs and Baer (1999). Because of the localized pressure rises seen when the reaction passes a transducer, the system was thought of as small cross-sections of material burning in a nearly constant volume. Therefore, the calculations were performed assuming a constant volume. The calculations included the $Al_2O_3$ from the passivation layers and the interstitial air, but did not include the effect of heat loss through the walls.

It was reasonable to neglect the heat loss because the time scale for conduction through the acrylic tube, $\tau_{loss}$, was much greater than the time for the reaction to propagate through all of the material, $\tau_r$. The time scale for heat loss was defined as $L^2/\alpha_{acr} = 80\,s$, where L is the length scale for conduction defined as the wall thickness of the tube, 3.2 mm, and $\alpha_{acr}$ is the thermal diffusivity of acrylic, $0.137\,mm^2/s$. The time for the reaction to propagate through all of the material was $L_{tube}/v_r = 127\,\mu s$, where $L_{tube}$ is the length of the tube (8.9 cm) and $v_r$ is the velocity of the reaction wave ($\sim 650\,m/s$).

Figure 11 shows the calculations and averaged experimental values for peak pressure as the weight percent of $Al_2O_3$ increased. There was a fair agreement between calculations and experiments, which gave a first order validation to these calculations and allowed them to be used to help interpret some results. Figure 12 shows the adiabatic flame temperature as a function of the weight percentage of $Al_2O_3$. As expected, adding $Al_2O_3$ decreases the adiabatic temperature.

To understand the primary mechanism for propagation, the calculated product concentrations and their phases were examined. The concentrations of the primary products as a function of $Al_2O_3$ concentration are shown in Figure 13. Even though most of the products were in the condensed phase, the depletion of the gas phase products (bottom half of Fig. 13) was what most effected the propagation. Examination of the total gas phase products showed an 82% decrease to a mole fraction of 0.004 when increasing from 0% to 20% $Al_2O_3$.

Furthermore, at values above 15% $Al_2O_3$, the equilibrium results suggest that the nAl reacted with the interstitial air to form solid AlN, thus removing some of the initial interstitial gas from the system. These results further suggest that the addition of $Al_2O_3$ lowered the flame temperature, which demoted gas production, as well as the overall energy release rate, and began to remove interstitial gases from the system, lowering the pressure and, thus, hindering the convective mode of heat transfer.

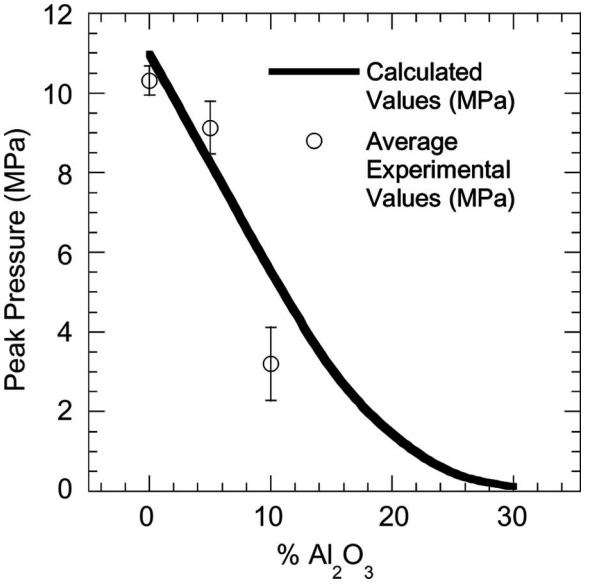


**Figure 11** Comparison of average experimental peak pressure values in the burn tube to the calculations for the peak pressure with added $Al_2O_3$ percentage for constant volume explosion.

Since convection was the primary propagation mechanism for this system, the reaction velocity decreased drastically and eventually became unstable at 20% $Al_2O_3$ where gaseous species were almost non-existent.

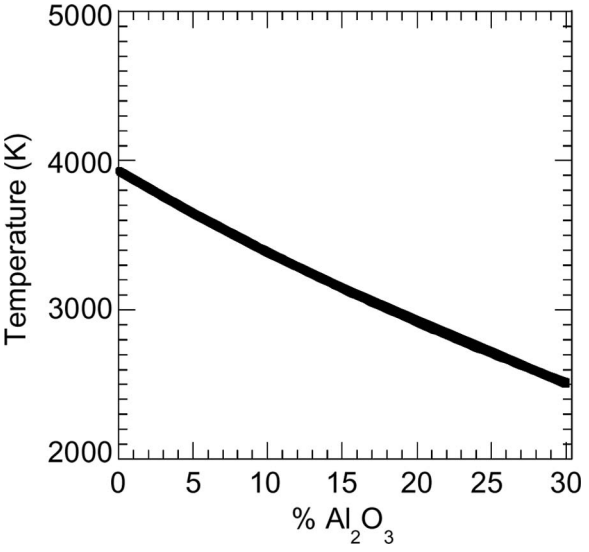


**Figure 12** Calculated adiabatic flame temperature as a function of added $Al_2O_3$ percentage for constant volume explosion calculations.

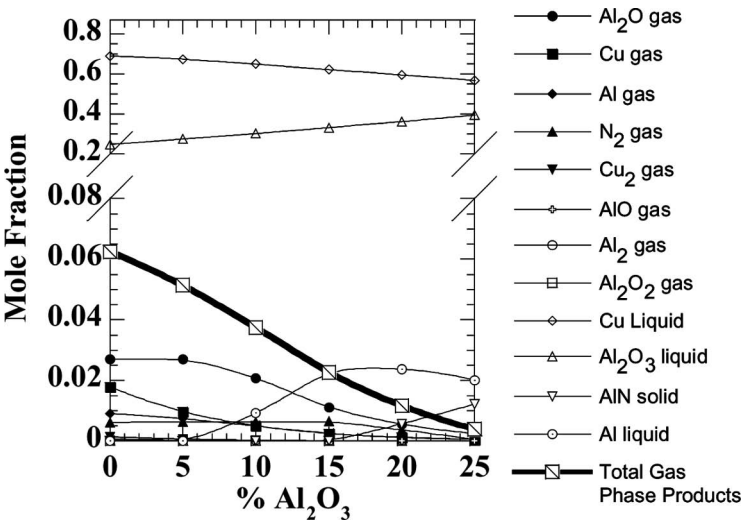


**Figure 13** Product concentrations versus $Al_2O_3$ percentage for constant volume calculations.

## CONCLUSIONS

This work focused on the effects of dilution of an Al/CuO nano-scale thermite with $Al_2O_3$ nano-particles. These solid phase end-products acted as a heat sink, which reduced combustion temperatures. This, in turn, hindered gas production and decreased the overall effect of the convective propagation mechanism. Three tests were performed to examine how propagation velocities and pressure output varied as a function of diluent ($Al_2O_3$ nano-particles) concentration. The pressure cell and burn tray were unconfined tests while the burn tube confined the material laterally.

The pressure cell showed a dramatic drop in peak pressure and rate of pressure rise when only 5% $Al_2O_3$ was added to the system. Moreover, the induction time drastically increased when the $Al_2O_3$ concentration exceeded 5%. These trends suggested that the addition of $Al_2O_3$ nanoparticles hindered the gases produced by combustion. The peak pressure trend corresponded directly with the two-point velocities found on the burn tray, which gave evidence that hindered gas production decreased the reaction velocity.

In the instrumented burn tube, the peak pressures were recorded as the reaction wave propagated through the material. These pressure traces demonstrated a clear dropoff as $Al_2O_3$ concentration increased, eventually showing relatively no pressure increase at 20% $Al_2O_3$. Furthermore, the propagation velocity changed from a steady rate of $\sim$650 m/s for 0% and 5% $Al_2O_3$ to an unsteady velocity (constant acceleration) regime for 10% and 15% $Al_2O_3$, and finally became unstable at 20% $Al_2O_3$.

The unstable regime at 20% $Al_2O_3$ initially showed an extremely slow propagation that eventually transitioned into a spiraling propagation through the material. Similar spiraling phenomena were observed with micron-scale thermites when a diluent was added to the system (Munir and Anselmi-Tamburini, 1989).

This change in propagation behavior and pressure output in the burn tube with added diluent was interpreted utilizing the results from equilibrium calculations. The peak pressures predicted by constant volume calculations matched well with the peak pressures recorded experimentally in the burn tube for each diluent concentration. Therefore, these types of calculations were used throughout to explain other phenomena.

Calculations showed the total gas production dropping 82% to a mole fraction of 0.004 when increasing from 0% to 20% $Al_2O_3$. This drastic depletion in gaseous species predicted by the calculations at 20% $Al_2O_3$ correlated well with the experimental propagation behavior. The reaction front drastically decreased in velocity and eventually demonstrated a spiraling combustion instability. This instability was a direct result of the primary mode of heat transfer, convection, being prohibited.



## REFERENCES


Asay, B.W., Son, S.F., Busse, J.R., and Oschwald, D.M. (2004) Ignition characteristics of metastable intermolecular composites. *Prop. Exp. Pyro.*, **29**(4), 216–219.

Begley, S.M. and Brewster, M.Q. (2007) Radiative properties of $MoO_3$ and Al nanopowders from light-scattering measurements. *J. Heat Trans.*, 05–1167 (in publication).

Bockmon, B.S., Pantoya, M.L., Son, S.F., Asay, B.W., and Mang, J.T. (2005) Combustion velocities and propagation mechanisms of metastable interstitial composites. *J. App. Phy.*, **98**, 064903.

Ershov, A.P., Kupershtokh, A.L., and Medvedev, D.A. (2001) Simulation of convective detonation waves in a porous medium by the lattice gas method. *Comb. Exp. Shock Waves*, **37**(2), 206–213.

Foley, T.J., Pacheco, A.N., Sanders, V.E., Son, S.F., and Asay, B.W. (2006) The effect of added alumina on the propagation behavior of the nanoaluminum and molybdenum (VI) oxide system. *13th Int. Det. Symp.*, 1217–1228.

Fried, L.E., Glaesemann, K.R., Howard, W.M., Souers, P.C., and Vitello, P.A. (2004) *Cheetah 4.0*, Lawrence Livermore National Laboratory, Livermore, CA.

Hobbs, M.L., Baer, M.R., and McGee, B.C. (1999) JCZS: An intermolecular potential database for performing accurate detonation and expansion calculations. *Prop. Exp. Pyro.*, **24**(5), 269–279.

Kuo, K.K., Chen, A.T., and Davis, T.R., Convective burning in solid propellant cracks. *AIAA Journal*, **16**(6), 600–607.

Mang, J.T., Hjelm, R.P., Son, S.F., Peterson, P.D., and Jorgensen, B.S. (2006) Characterization of components of nano-energetics by small-angle scattering techniques. *J. Mat. Res.*, **22**(7), 1907–1920.

Munir, Z.A. and Anselmi-Tamburini, U. (1989) Self-propagating exothermic reactions: the synthesis of high-temperature materials by combustion. *Mat. Sci. Repts.*, **3**(7–8), 277–365.

Naud, D.L., Hiskey, M.A., Son, S.F., Busse, J.R., and Kosanke, K. (2003) Feasibility study on the use of nanoscale thermites for lead-free electric matches. *J. Pyrotechn.*, **17**, 201–211.

Pantoya, M.L., Son, S.F., Danen, W.C., Jorgensen, B.S., Asay, B.W., and Busse, J.R. (2004) Defense applications of nanomaterials. In Miziolek, A.W., et al. (Ed.) *Characterization of Metastable Intermolecular Composites (MICs)*, ACS Symposium Series Book, Chap. 16, Vol. 3.

Pantoya, M.L. and Granier, J.J. (2005) Combustion behavior of highly energetic thermites: nano versus micron composites. *Prop. Exp. Pyro.*, **30**(1), 53–62.

Perry, W.L., Smith, B.L., Bullion, C.J., Busse, J.R., Macomber, C.S., Dye, R.C., and Son, S.F. (2004) Nano-scale tungsten oxides for metastable intermolecular composites. *Prop. Exp. Pyro.*, **29**(2), 99–105.

Sanders, V.E., Asay, B.W., Foley, T.J., Tappan, B.C., Pacheco, A.N., and Son, S.F. (2006) Combustion and reaction propagation of four nanoscale energetic composites. *33rd Int. Pyro. Sem.*, 113–121.

Son, S.F. and Brewster, M.Q. (1995) Radiation augmented combustion of homogeneous solids. *Combust. Sci. Technol.*, **107**, 127.

Varma, A. and Lerat, J.P. (1992) Combustion synthesis of advanced materials. *Chem. Eng. Sci.*, **17**(9–11), 2179–2194.

Wang, L.L., Munir, Z.A., and Maximov, Y.M. (1993) Thermite reactions: their utilization in the synthesis and processing of materials. *J. Mat. Sci.*, **28**, 3693.